Stem Cell Research & Therapy

RESEARCH

Open Access

Highly efficient generation of mature megakaryocytes and functional platelets from human embryonic stem cells

Chuxin Chen[1,2†], Ning Wang[1,2†], Xueyan Zhang[1,2†], Yingjie Fu[1,2†], Zhiyong Zhong[2], Haibin Wu[1,2], Yaming Wei[3*] and Yuyou Duan[1,3,4,5*]

Abstract

Background Platelet transfusion therapy has made a great breakthrough in clinical practice, and the differentiation of human embryonic stem cells (hESCs) to produce functional platelets has become a new potential approach, however, efficient generation of functional platelets still faces great challenges. Here, we presented a novel approach to highly and efficiently generate mature megakaryocytes (MKs) and functional platelets from hESCs.

Methods In hypoxic conditions, we successfully replicated the maturation process of MKs and platelets in a controlled in vitro environment by introducing an optimal combination of cytokines at various stages of development. This method led to the generation of MKs and platelets derived from hESCs. Subsequently, mature MKs and functional platelets were further comprehensively investigated and characterized using a variety of methodologies, including flow cytometry analysis, RT-qPCR validation, Giemsa-Wright's staining, immunofluorescent staining, RNA transcriptome analysis, and DNA ploidy analysis. Additionally, the in vivo function of platelets was evaluated through the transplantation using thrombocytopenia model mice.

Results Under our 3D differentiation conditions with four sequential stages, hESCs could be efficiently induced into mature MKs, with 95% expressing CD41aCD42a or 90% expressing CD41aCD42b, and those MKs exhibited polyploid properties, produced filamentous proplatelet structures and further generated platelets. Furthermore, 95% of platelets showed $CD42b^{+}CD62p^{+}$ phenotype upon the stimulation with ADP and TRAP-6, while 50% of platelets exhibited the ability to bind PAC-1, indicating that hESC-derived platelets possessed the in vitro functionality. In mice models of thrombocytopenia, hESC-derived platelets effectively restored hemostasis in a manner comparable to human blood-derived platelets. Further investigation on the mechanism of this sequential differentiation revealed that cellular differentiation and molecular interactions during the generation of hESC-derived MKs and platelets recapitulated the developmental trajectory of the megakaryopoiesis and thrombopoiesis.

Conclusions Thus, our results demonstrated that we successfully established a highly efficient differentiation of hESCs into mature MKs and functional platelets in vitro. The in vivo functionality of hESC-derived platelets closely

†Chuxin Chen, Ning Wang, Xueyan Zhang and Yingjie Fu have equally contributed to this work.

*Correspondence:
Yaming Wei
eywym@scut.edu.cn
Yuyou Duan
yuyouduan@scut.edu.cn
Full list of author information is available at the end of the article

resembles that of natural human platelets, thus offering a promising avenue for the development of functional platelets suitable for future clinical applications.

Keywords Human embryonic stem cells, Mesoderm, Hematopoietic stem/progenitor cells, Megakaryocytes, Platelets, Directed differentiation

Introduction

Platelets play a central role in the thrombosis and hemostasis, thus platelet transfusion provides an important therapeutic intervention in the treatment or prevention of thrombocytopenia or platelet dysfunction [1–6]. With the increasing demand for transfusion, however, donor-dependent platelet transfusions are associated with practical problems, such as limited supply [7]. To overcome this problem, much efforts have been made to generate in vitro-based platelets. Human pluripotent stem cells (hPSCs) may serve as an alternative source of platelets for replacement transfusion. Mature megakaryocytes and functional platelets in vitro were successfully generated in vivo using hESCs co-cultured with stromal cells [8]. Similarly, by enforcing the expressions of C-MYC, BMI1, and BCL-XL transcription factors [9], or GATA1, FLI1, and TAL1 transcription factors [10], induced pluripotent stem cells (iPSCs) were successfully induced into mature megakaryocytes and obtained functional platelets. However, the introduction of exogenous stromal cells and the accuracy of gene editing remain a concern for clinical applications. Therefore, efficient generation of functional platelets with clinical potential from hPSCs faces a great challenge.

The megakaryopoiesis is a highly complex process that requires synergy between a wide range of cell types. Megakaryocytes (MKs) are produced in bone marrow by sequential differentiation from hematopoietic stem cells (HSCs), under the control of a variety of growth factors and transcription factors. Hematopoietic stem/progenitor cells (HSPCs) first directly differentiate into common lymphoid progenitors (CLPs) or common myeloid progenitors (CMPs), the latter of which give rise to MK-erythrocyte progenitors (MEPs), which show bipotent cells that bifurcate to lineage-committed MKs and erythroid cells [11–14]. Previous studies have shown that the development of MKs is tightly regulated by both cell-intrinsic and cell-extrinsic mechanisms involving cytokines and transcription factors as well as epigenetic regulation. For instance, thrombopoietin (TPO) is a critical regulator of the megakaryopoiesis, which signals via its receptor MPL (TPO-R) to promote the proliferation of megakaryocyte progenitors (MKPs) and the maturation of MKs. As for other factors, such as transcription factor FLI1, it has been implicated in the terminal maturation of MKs, and its overexpression inhibits erythroid development, driving cell lines to develop megakaryocytic features. According to the current model of the megakaryopoiesis, terminal maturation of MKs is coordinated with localization at vascular sinusoidal niches within bone marrow, through which they extend and sequentially release platelets into the circulation. In terms of MK fates, a range of cell surface markers, including CD41a and CD61 [15], are characterized during early-phase megakaryocytopoiesis. The sequential increased the expression of cell surface molecules CD42a, CD42b and CD42d, are accompanied, all of those markers are the most abundant as MKs are matured [16]. At least three distinct developmental types of mature MK have been identified in the human body, which respectively regulate the maintenance of HSCs, immune response, and platelet production [17, 18]. Among them, thrombocytogenic MKs are terminally large polyploidy cells derived from hematopoietic cells, whose nucleus becomes multilobed by the endomitosis, together with an enlargement of the cytoplasm, which becomes filled with platelet-specific granules and thereby responsible for platelet production [19, 20]. Nowadays, expandable MK lines derived from hPSCs are considered suitable as master cells for producing platelets, since they offer the advantages of unlimited expansion in culture and are amenable to genetic manipulation [21]. While effective, however, it is difficult to produce large-scale quantities of MKs and platelets for clinical use via this method [22, 23].

Consequently, we presented a novel, stepwise, completely xeno-free and defined culture method which enabled robust generation of MKs from hESCs by utilizing 3D differentiation system. Compared with previous methods using a 2D culture system or relying on gene editing and heterogeneous cell co-culture, our 3D culture method was closer to natural environment of MKs in vivo, which not only improves the generation efficiency of MKs, but also reduces the safety concerns associated with exogenous gene manipulation and heterogeneous cell co-culture. These properties make the method more advantageous for potential clinical applications. Here, 3D induction mode involved generating spheroids under the hypoxia conditions (5% O_2), followed by culture in specific in vitro conditions to induce further differentiation of MKs and platelets. By strictly mimicking the in vivo development of MKs and platelets, we presented that the sequential differentiation of hESCs were induced

at different stages. This led to the generation of immature MKs, which further matured with unique features such as large size and polyploidism. These characteristics potentially indicated a propensity for more efficient platelet production and release. Then the in vitro function of these hESC-derived platelets was evaluated by the activation with ADP and TRAP-6. Furthermore, the restoration of hemostasis in vivo was determined by the infusion of hESC-derived platelets into the developed thrombocytopenic mice, finally the mechanism by which the megakaryopoiesis and thrombopoiesis were further investigated during the sequential differentiation of hESCs towards MKs and platelets.

Methods

Detail methods and materials are provided in the Supplementary Materials.

Results

Early hematopoietic lineage commitment from hESCs

Hypoxia is considered to be a significant promoter to drive the hematopoiesis [24, 25]. Since MKs are originated from HSC–derived bipotent MEPs during the hematopoiesis, thus, in the present study, hypoxic condition was used as the culture condition, which would promote hematopoietic commitment and definitive hematopoiesis, in turn facilitate the production of megakaryocytic cells. To explore the regulatory process of the differentiation of hESCs towards MKs, we developed a four-stage differentiation approaches under 3D culture conditions, which strictly mimicked the in vivo development of MKs and platelets (Fig. 1A). Briefly, hESCs underwent a two-day differentiation into mesodermal progenitor cell (MPC) spheroids in a 3D state, followed by an additional four days of differentiation to form hematopoietic endothelial cell (HEC) spheroids. These HEC spheroids generated early hematopoietic cells, and on the ninth day of the differentiation, MEPs were produced as individual suspension cells (Fig. 1A, Figure S1). Afterward, these MEPs entered the MK differentiation stage (the first day of MK differentiation was defined as day 9 + 0), and differentiated into early MKs at day 9 + 2, further developed into mature MKs at day 9 + 6, and eventually produced platelets (Fig. 1A, Figure S1). Since both waves of the hematopoiesis were originated from the lateral plate mesoderm and endothelial lineages [26], in our study, we induced mesoderm differentiation with BMP4, Activin A and WNT inhibitor CHIR99021 under serum-free conditions over a 2-day period (Fig. 1A), thus, we first analyzed the relative expression of mesodermal genes and pluripotent genes. The results indicated that the Brachyury was highly expressed at day 2 and down-regulated overtime while pluripotent genes OCT4 and SOX2 were dramatically decreased in both the derivatives of H9 and H1 cells (Fig. 1B, Figure S2, S3), mimicking the process of in vivo mesodermal development. In subsequent stage, cells with mesoderm lineage cultured in the presence of VEGF and bFGF acquired the expression of transcription factor KDR (Fig. 1B, C), indicating the emergence of HECs. Then, the developing HEC spheroids led to hematopoietic fate by highly expressing the hematopoietic endothelium genes (VE-Cadherin/CD144, CD34, SOX17 and CD31), early hematopoietic transcription factors (ERG and TIE1), and hematopoietic genes (CD43 and CD45) (Fig. 1B, C, Figure S2). Moreover, these results were also independently verified by flow cytometry. Over 40% $CD31^+CD34^+$ HECs and a very small number of $CD43^+$ hematopoietic cells were recognized at day 6 (Fig. 1C, Figure S4). Consistently, immunofluorescence staining also showed CD43 positive cells in the HEC spheroids at day 6 (Fig. 1D), which represented the production of early hematopoietic cells [27].

To analyze genes involved in the differentiation of hESCs into hematopoietic cells at different stages, H9 hESCs, MPC spheroids at day 2 and HEC spheroids at day 6 were collected and a whole-genome transcriptome

(See figure on next page.)

Fig. 1 Identification of hematopoietic specification during the differentiation of hESCs. **A** Differentiation scheme of MKs and platelets derived from hESCs. **B** RT-qPCR analysis for the expression of mesodermal genes (Brachyury and KDR), endothelial gene (VE-Cadherin, SOX17, CD31) and hematopoietic genes (CD34, ERG, TIE1, CD43 and CD45) in different cell populations during the hematopoietic specification of H9 hESCs (n = 3). Data represent the means ± SD. *$p < 0.05$, **$p < 0.01$, ***$p < 0.001$ and ns (no significance). **C** Flow cytometry was performed to determine the generations of KDR^+ hematopoietic mesoderm, $CD31^+CD34^+$ hematopoietic endothelial cells and $CD43^+$ early hematopoietic cells from H9 hESCs at days 0, 2, 4 and 6 employing hematopoietic differentiation protocol. **D** CLSM images of co-immunostaining for α-tubulin and CD43 in the differentiated cells at day 6 after the differentiation of H9 hESCs. The colors of green, red and blue represented the staining for α-tubulin, CD43 and nuclei, respectively. (Original magnification, 40x, Scale bar, 100 μm). **E** The volcano plot showed the distribution trends for DEGs between the cells from H9 hESCs at days 0 and 2 (Red spots represented up-regulated genes; blue spots represented down-regulated genes) and non-DEGs (gray spots). **F** GO terms were enriched in the up-regulated genes at day 2 after the differentiation of H9 hESCs. **G** The volcano plot showed the distribution trends for DEGs between the cells from H9 hESCs at days 2 and 6 (Red spots represented up-regulated genes; blue spots represented down-regulated genes) and non-DEGs (gray spots). **H** GO terms were enriched in the up-regulated genes at day 6 after the differentiation of H9 hESCs

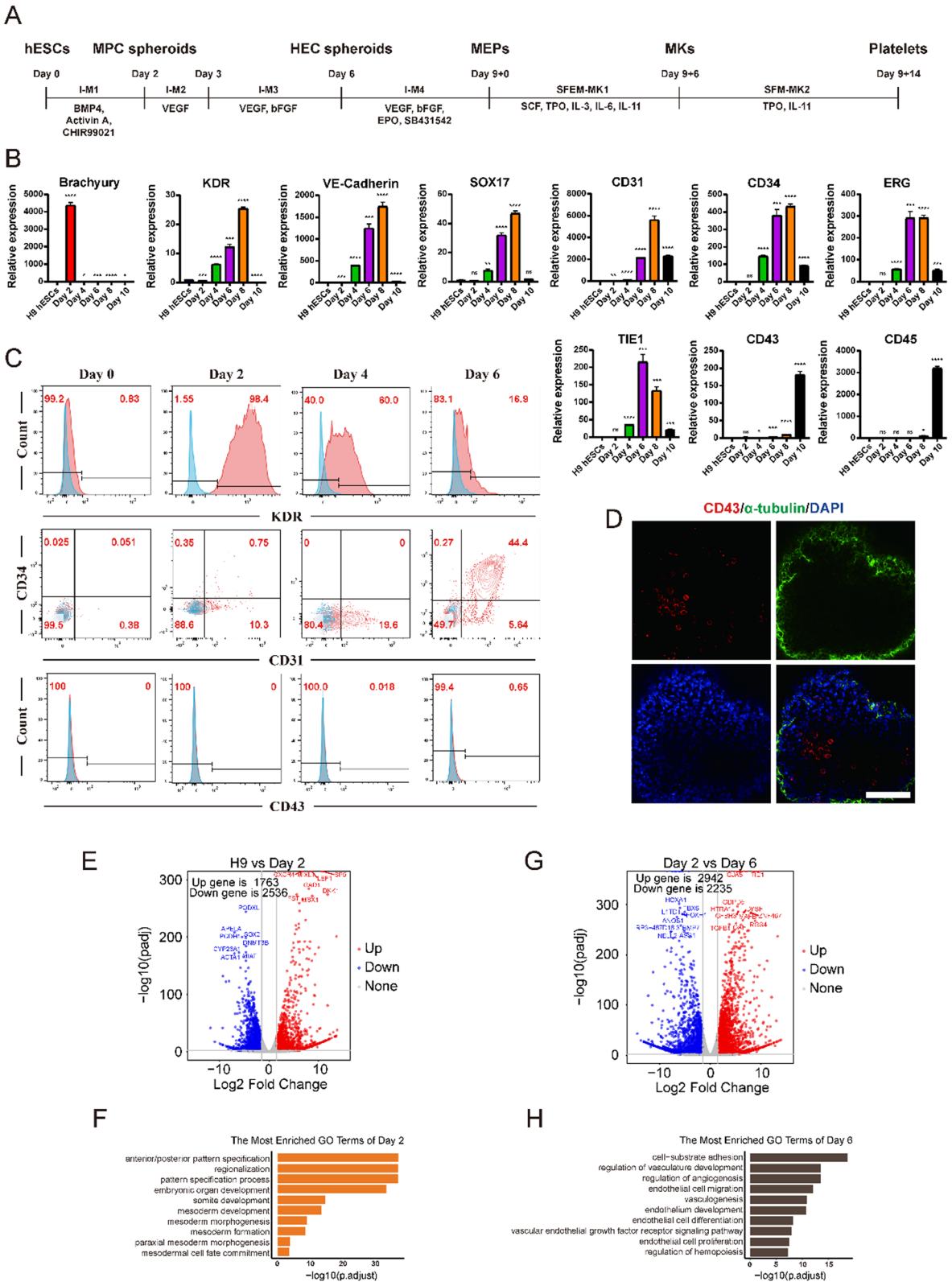

Fig. 1 (See legend on previous page.)

analysis was performed. The results showed that the expression level of the genes among them was significantly different (Figure S5). Compared with undifferentiated H9 hESCs, 1763 differentially expressed genes (DEGs) were upregulated and 2536 DEGs were downregulated in MPC spheroids at day 2 (Fig. 1E). Among them, MIXL1 (related to mesoderm), LEF1 and SP5 (related to WNT signaling pathway), FST (related to Activin signaling pathway) were up-regulated, droving them to acquire mesodermal properties (Fig. 1E). Gene enrichment analysis of those 1763 up-regulated DEGs revealed the involvement of embryonic organ development, mesoderm development and mesoderm morphogenesis at day 2 (Fig. 1F). Compared with MPC spheroids at day 2, we further identified 2942 up-regulated DEGs and 2235 down-regulated DEGs in HEC spheroids at day 6, including FOXH1 and TBX6 (down-regulated) related to mesoderm development and TIE1 and GJA5 related to endothelial development and angiogenesis (Fig. 1G). To explore the biological function of DEGs, gene ontology (GO) enrichment analysis was performed and showed that HEC spheroids at day 6 were mainly involved in the biological processes of regulation of angiogenesis, endothelial cell development and differentiation as well as regulation of hemopoiesis (Fig. 1H). In summary, these results indicated that under our 3D culture conditions, hESCs successfully differentiated into HEC spheroids, and these HECs possessed the ability to transform into hematopoietic cells.

Differentiation of early hematopoietic cells towards MK-erythrocyte progenitors (MEPs)

Erythropoietic growth factor EPO plays an important role in the development of MEPs, $CD31^+CD34^+$ HECs can indeed be diverted towards $CD235a^+CD41a^+$ MEPs fate in vitro upon EPO-stimulation [14]. A number of studies have shown that the TGF-β signaling pathway is essential for the development of MPCs, but negatively regulate the endotheliogenesis and endothelium-hematopoietic transformation (EHT) during the embryonic hematopoiesis [28]. The inhibitor SB431542 can significantly increase the number of $CD31^+CD34^+$ HECs and contribute to effective hematopoiesis after the induction of mesoderm by blocking TGF-β signaling pathway [28–31]. Accordingly, we established two differentiation approaches with different conditions (designated as I-M4 and I-M5 conditions respectively) to drive the megakaryopoiesis (Fig. 2A). Under these two conditions, there were more MEP suspended cells generated from the HEC spherioids after 3 days' culture (Figure S6). In order to verify the induction efficiency of I-M4 or I-M5 conditions, we first quantified the proportions of $CD43^+$ cells and $CD235a^+CD41a^+$ cells in HEC spheroids at day 9 by flow cytometry. Under I-M4 condition, the proportion of $CD43^+$ cells (about 10%) and $CD235a^+$ $CD41a^+$ cells (about 2%) was small; under I-M5 condition, the proportion of $CD43^+$ cells and $CD235a^+CD41a^+$ cells (about 15% and 3%) was also low (Fig. 2B), suggesting no significant difference between the two conditions at this stage. However, we observed higher expression level of erythroid-related gene (KLF1) in I-M5 conditions than those in I-M4 conditions (Fig. 2C). Interestingly, the expression levels of MK-related genes, such as GATA1, RUNX1 and FLI1, were also highly expressed in HEC spheroids cultured in I-M5 condition (Fig. 2C). Since MEP suspension cells were generated from HEC spheroids at high efficiency, we thus also tested their characteristics. Flow cytometry analysis showed that the proportions of $CD43^+$ cells in MEP suspension cells at day 9 + 0 produced under both I-M4 and I-M5 conditions were similar (over 95%), meanwhile the proportion of $CD235a^+CD41a^+$ cells under I-M4 conditions was higher than that under I-M5 conditions (Fig. 2D). Moreover, RT-qPCR analyses showed the expression levels of KLF1 and GATA1 in MEP suspended cells at day 9 + 0 under I-M5 conditions was lower, but the expression levels of RUNX1 and FLI1 were higher (Fig. 2E). Therefore, those results showed that I-M4 was more conducive to the production of $CD41a^+$MEPs (Fig. 2B–E).

We next performed differential expression analysis to further investigate the transcriptional differences between HEC spheroids at day 6 and 9. There were

(See figure on next page.)

Fig. 2 Identification of MEP specification of early hematopoietic cells derived from hESCs. **A** MEPs were produced from early hematopoietic spheroids employing two different induction mediums (I-M4 and I-M5). **B** The proportions of $CD43^+$cells and $CD235a^+CD41^+$cells from hematopoietic spheroids from H9 hESCs at day 9 were determined by flow cytometry under I-M4 or I-M5 induction medium (n = 3). **C** Expression analysis of erythroid-related gene (KLF1) and MK-related genes (GATA1, RUNX1 and FLI1) in hematopoietic spheroids from H9 hESCs by RT-qPCR (n = 3). **D** The proportions of $CD43^+$ hematopoietic cells and $CD235a^+CD41a^+$ MEPs in suspension cells from H9 hESCs were determined by flow cytometry under I-M4 or I-M5 induction medium (n = 4). **E** Gene expression analysis for erythroid-related gene (KLF1), and MK-related genes (GATA1, RUNX1 and FLI1) in suspension cells from H9 hESCs by RT-qPCR (n = 3). **F** The volcano plot showed the distribution trends for DEGs between the cells at days 9 and 6 (Red spots represented up-regulated genes; blue spots represented down-regulated genes) and non-DEGs (gray spots). **G** GO terms were enriched in the up-regulated genes at day 9 after the differentiation of H9 hESCs. All data in B, C, D, E were represented as means ± SD. *$p < 0.05$, **$p < 0.01$, ***$p < 0.001$ and ns (no significance)

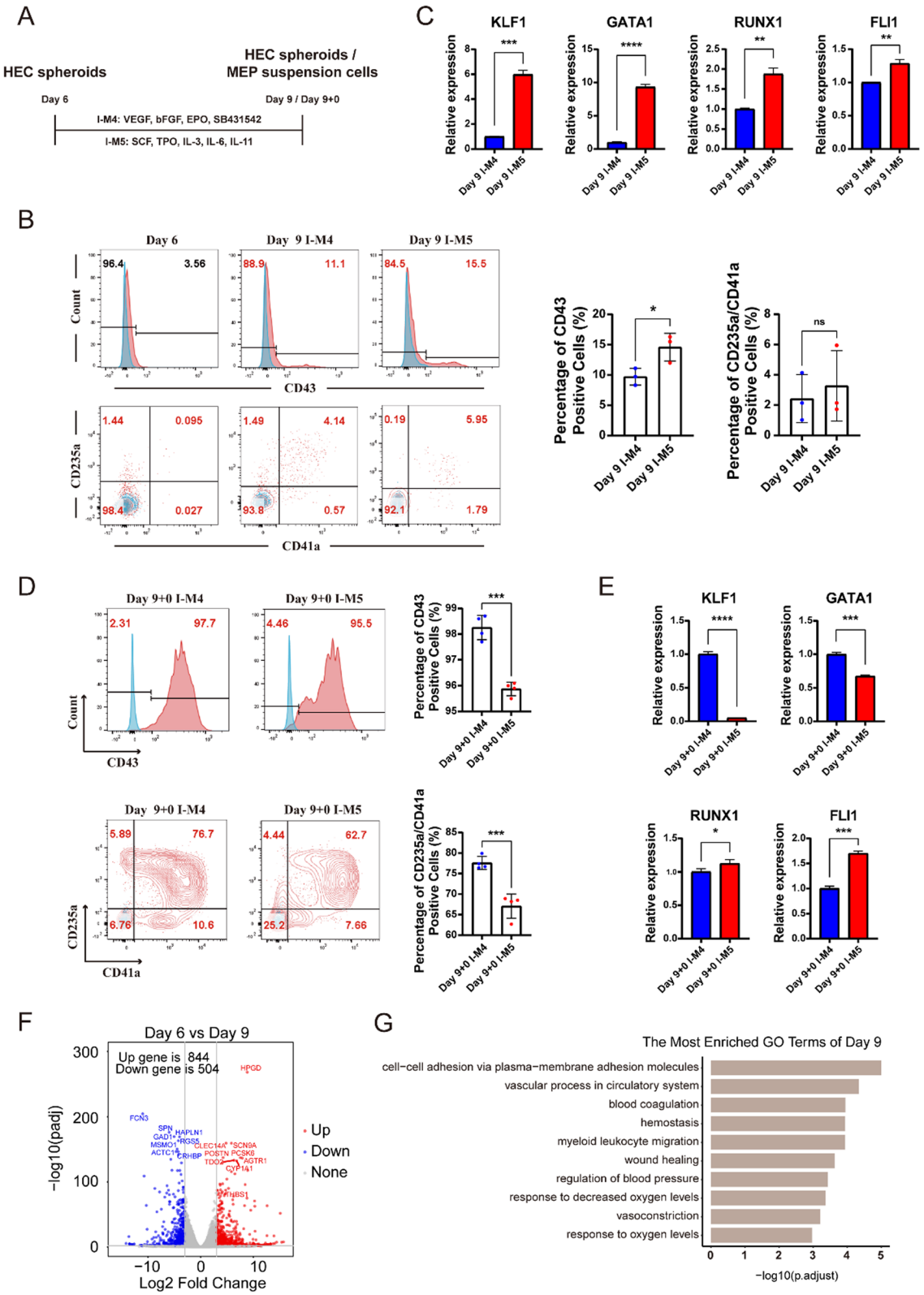

Fig. 2 (See legend on previous page.)

significant differences in gene expression levels between HEC spheroids at day 6 and day 9 (Figure S7), with 504 down-regulated DEGs and 844 up-regulated DEGs at day 9 (Fig. 2F). Interestingly, THBS1, a characteristic of HECs with a bias towards MK lineage differentiation [32], was also upregulated. Using GO enrichment, we found that HEC spheroids at day 9 were mainly involved in biological processes related to cell–cell adhesion via plasma-membrane adhesion molecules, vascular process in circulatory system and blood coagulation (Fig. 2G). In general, these results indicated that the hESC-derived HEC spheroids could generate early hematopoietic cells and subsequently differentiated towards MEP suspension cells.

HEC spheroids could be maintained and continuously produced MEP suspension cells

Several studies have shown that during the erythropoiesis, MEPs could be maturated into erythrocytes with the continuous stimulation of EPO [33]. However, there was also obvious evidence that HECs could be differentiated into $CD235a^+CD41a^+$ MEPs under short-term induction (about 2 days) by EPO [14]. Therefore, we explored whether I-M4 medium supplemented with EPO was still suitable for the subsequent culture of HEC spheroids. In our study, HEC spheroids cultured with I-M4 medium from day 6 to 9 were isolated from MEP suspension cells, and then cultured with I-M4 or I-M5 mediums for 3 more days respectively (Fig. 3A). After 3 days' induction, HEC spheroids could still produce MEP suspended cells under both I-M4 and I-M5 conditions. Using flow cytometry, we found that the percentages of $CD43^+$ cells and $CD235a^+CD41a^+$ cells in HEC spheroids at day 12 remained at a low level in both I-M4 and I-M5 conditions, and the percentages of $CD235a^+CD41a^+$ cells in I-M5 were slightly higher than that in I-M4 (Fig. 3B). For the newly-generated MEP suspended cells (at day 12 + 0) induced by I-M5 medium, up to 90% of cells were positive for CD43, which significantly higher than those by I-M4 condition (Fig. 3C). Moreover, we found that a larger proportions of $CD235a^+CD41a^+$ cells (more than 65%) were also induced by I-M5 condition, significantly higher than those by I-M4 (about 30%) (Fig. 3C). Consistently, the percentages of $CD41a^+$ suspension cells (at day 12 + 0) in I-M5 induction medium were significantly higher than those in I-M4 condition (Fig. 3D). Meanwhile, RT-qPCR results showed that the gene expression levels of erythroid specific transcription factor KLF1 and TAL1 in HEC spheroids at day 12 were significantly higher in I-M4 medium (Fig. 3E), while MK specific transcription factors FLI1 and GATA1 were highly expressed in I-M5 medium (Fig. 3E). In addition, compared with I-M5 medium, the MEP suspension cells (at day 12 + 0) induced by I-M4 medium significantly expressed TAL1 and KLF1 at high levels as well (Fig. 3F), though the expression levels of megakaryocytic specific transcription factors RUNX1, FLI1 and GATA1 in those two conditions were no significant (Figure S8). Then we further evaluated the gene expression levels of platelet-specific transcription factors in the MEP suspension cells (at day 12 + 0) from these two conditions. When compared with I-M4 medium, the MEP suspension cells (at day 12 + 0) induced by I-M5 medium expressed significantly higher levels of PF4, NFE2, FOG1 and β1-tubulin (Fig. 3F). Therefore, these results indicated that I-M5 medium was more suitable to subsequently generate MEP suspended cells biased toward the megakaryocytic lineage.

In order to further investigate whether HEC spheroids induced by I-M5 medium (after day 9) could be maintained and continuously produce MEP suspended cells biased toward the megakaryocytic lineage, which is essential for mass in vitro platelet production. The HEC spheroids induced by I-M4 medium from day 6 to 9 and then by I-M5 medium from day 9 to 12 were isolated, and subsequently maintained in fresh I-M5 medium. After 9 more days of the cultivation, those HEC spheroids remained the 3D shape, but their sizes became smaller (Figure S9), probably due to continuing to produce MEP suspension cells. Starting at day 9, suspension cells were collected every 3 days, and the number of newly-generated suspended cells were gradually increased and peaked at day 18, then the number began to decrease subsequently (Figure S10), indicating that HEC spheroids could be maintained and produced MEP suspended

(See figure on next page.)

Fig. 3 I-M5 medium condition was more suitable for HEC spheroids to generate MEP suspension cells at high efficiency. **A** MEP spheroids could be maintained in both I-M4 and I-M5 induction medium (Day 12 referred to cell spheroids, Day 12 + 0 referred to suspension cells). **B** Generation of $CD43^+$ hematopoietic cells and $CD235a^+CD41a^+$ MEPs in hematopoietic spheroids from H9 hESCs at day 12 were determined by flow cytometry under I-M4 or I-M5 medium (n = 3). **C** Representative flow cytometry results showed the populations of $CD43^+$ hematopoietic cells and $CD235a^+CD41a^+$ MEPs in suspension cells from H9 hESCs at day 12 in I-M4 or I-M5 medium (n = 4). **D** The percentages of $CD41a^+$ cells in suspension cells from H9 hESCs at day 12 in I-M4 or I-M5 under medium were quantitated (n = 3). **E** Expression analysis of erythroid-related gene (KLF1 and TAL1) and MK-related genes (FLI1 and GATA1) in hematopoietic spheroids from H9 hESCs by RT-qPCR (n = 3). **F** Expression analysis of erythroid-related genes (TAL1 and KLF1) and platelet-specific genes (PF4, NFE2, FOG1 and β1-tubulin) in suspension cells from H9 hESCs by RT-qPCR (n = 3). All data in B, C, D, E, F were represented as means ± SD. *$p < 0.05$, **$p < 0.01$, ***$p < 0.001$ and ns (no significance)

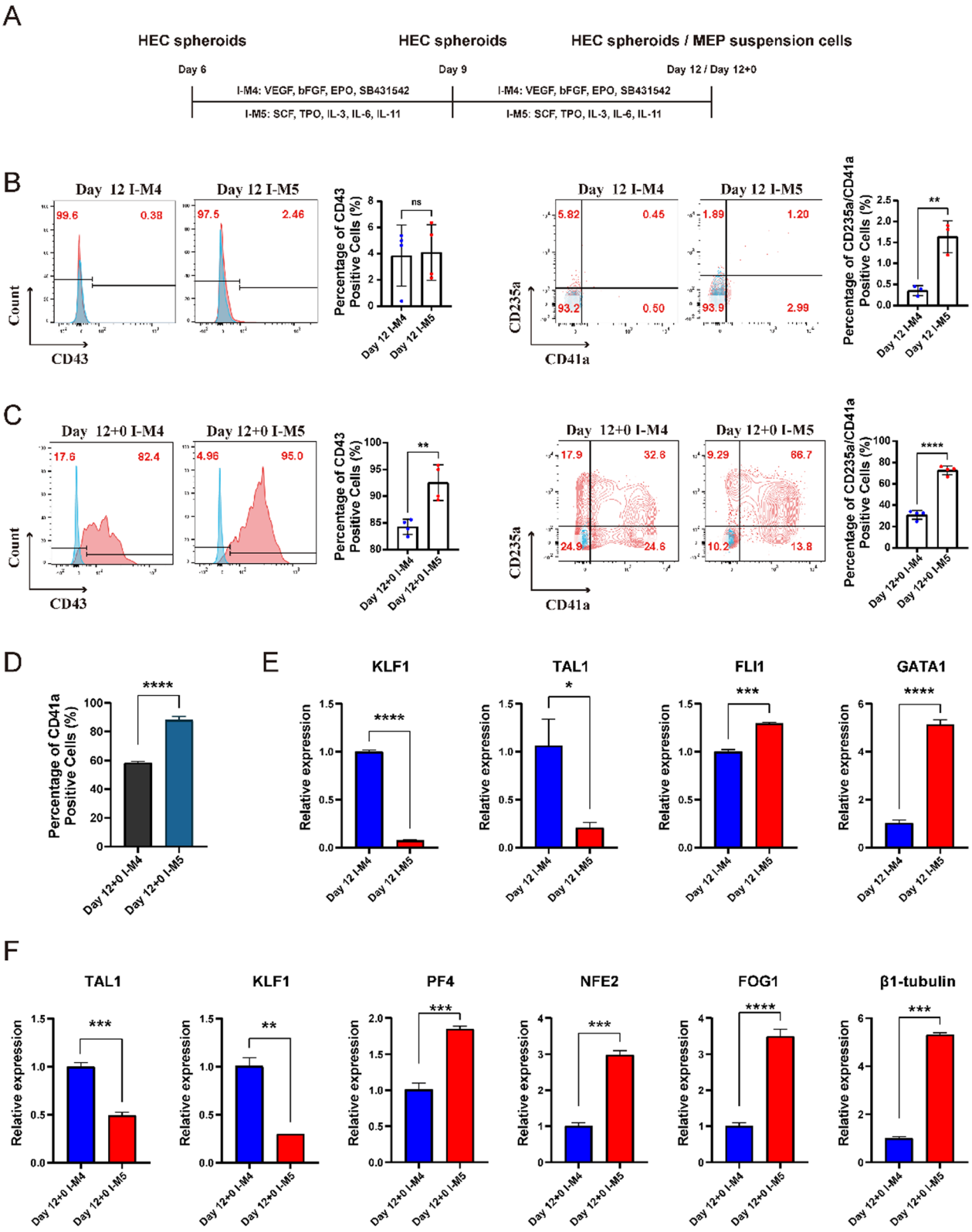

Fig. 3 (See legend on previous page.)

cells for a short period of time under I-M5 medium. Flow cytometry analysis at days 12, 15, 18 and 21 showed that 27%−55% of $CD31^+CD34^+$ HECs persisted in HEC spheroids, which peaked at day 15 (Fig. 4A). The percentages of $CD43^+$ cells were at a low level (less than 10%) before day 18, and then increased rapidly (more than 50%) (Fig. 4A). And consistent with the results of HEC spheroids at day 9, the proportions of $CD235a^+CD41a^+$ cells remained at a low level (less than 3%) (Fig. 4A). The analysis of gene expression pattern also showed that MK-specific genes FLI1, RUNX1 and GATA1 and erythroid specific genes KLF1 and TAL1 in HEC spheroids were dynamically changed and most of them reached the peak at day 15 (Fig. 4B). Flow cytometry analysis showed that more than 95% suspension cells (from days 12 + 0 to 21 + 0) generated from HEC spheroids at days 12 to 21 highly expressed CD43 (Fig. 4C), and the proportions of $CD235a^+CD41a^+$ cells were decreased rapidly after day 12 + 0, whereas the proportion of $CD41a^+$ cells maintained at more than 60% (Fig. 4C, D). This phenomenon might be due to the accelerated differentiation process to drive MEP suspension cells into MK lineage under the consecutive culture with I-M5 medium. The expression levels of MK-specific genes (RUNX1, GATA1 and FLI1) and erythroid specific genes (TAL1 and KLF1) as well as platelet-specific genes (NFE2, PF4, β1-tubulin and FOG1) in the MEP suspension cells were further evaluated and their genes expression dynamically changed, in which, the expressions of RUNX1, GATA1, NFE2, PF4 and β1-tubulin reached the peak at day 15 + 0, while the expressions of FLI1, TAL1 and KLF1 were decreased gradually (Fig. 4E). Collectively, the hESC-derived HEC spheroids could be maintained and continuously produced MEP suspension cells with MK potential under specific conditions.

Differentiation of MK progenitors into mature MKs

MEPs have bidirectional differentiation potentials with MK lineage and erythroid lineage, and can be labeled as $CD235a^+CD41a^+$ cells [34]. In our differentiation system, more than 76% $CD235a^+CD41a^+$ MEP suspension cells (at day 9 + 0) were produced from the HEC spheroids at day 9 after the differentiation in I-M4 medium (Fig. 2D). As shown in Fig. 5A, the MEP suspended cells at day 9 + 0 were collected and cultured with SFEM medium supplemented with SCF, TPO, IL-3, IL-6 and IL-11. During the 6-day differentiation process at this stage, flow cytometry analysis showed the percentages of $CD235a^+CD41a^+$ MEPs with a trend of first increase and then decrease (Fig. 5B), while a continuous rise of the proportions of $CD41a^+$ MKs maintained during this differentiation process (Fig. 5C), indicating that MEPs gradually changed their fate into MK lineage commitment. Moreover, CD42a (Glycoprotein IX Platelet, GP IX) and CD42b (Glycoprotein Ib Platelet Subunit Alpha, GP Ibα) is necessary components of GP Ib-IX-V complex, which can facilitate initial platelet adhesion to vascular sub-endothelium after vascular injury when binding to vWF (Von Willebrand Factor), and they are identified as surface markers for mature MKs [35]. During the induction of MK maturation, the proportions of $CD41a^+CD42a^+$ and $CD41a^+CD42b^+$ mature MKs were increased rapidly in the derivatives of both H1 and H9 cells (Fig. 5D, Figure S11). Notably, light microscopic observation revealed that filamentous proplatelet structures appeared on the surface of MKs at day 9 + 6 after MK differentiation (Figure S12). Since polyploidy is one of the important characteristics of mature MKs, we then analyzed DNA content of cells at this stage, and the results showed that 57%, 34% and 7% cells were at the 2N, 4N and 8N polyploid stage respectively, and over 1% were at the ≥ 16 N polyploid stage (Fig. 5E). Wright-giemsa staining further showed that hESC-derived MKs had multinucleated structures (Fig. 5F). Coincident with these aforementioned results, immunofluorescence staining further revealed high expression of CD62P in mature MKs (Fig. 5G), which is essential for platelet adhesion by binding to its counterpart P-selectin binding protein on neutrophils and endothelial cells and is considered a typical MK and platelet marker. Moreover, the expression of MK lineage specific markers (CD41a, CD42a, CD42b, CD62p) was increased gradually (Fig. 5H), MK-specific transcription factors (RUNX1, FEL1, GATA1,

(See figure on next page.)

Fig. 4 HEC spheroids could be maintained and generated single MEP suspended cells at high efficiency. **A** Generations of $CD31^+CD34^+$ HECs, $CD43^+$ hematopoietic cells and $CD235a^+CD41a^+$ MEPs in cell spheroids from H9 hESCs at days 12, 15, 18 and 21 were analyzed by flow cytometry. **B** Expression analysis of MK-related genes (FLI1, RUNX1 and GATA1) and erythroid-related genes (KLF1 and TAL1) in cells spheroids from H9 hESCs at days 12, 15, 18 and 21 by RT-qPCR (n = 3). **C** Generations of $CD43^+$ hematopoietic cells and $CD235a^+CD41a^+$ MEPs in hematopoietic suspension cells (at days 12 + 0, 15 + 0, 18 + 0 and 21 + 0) from H9 hESCs were determined by flow cytometry. **D** The percentages of $CD41a^+$ cells in hematopoietic suspension cells (at days 12 + 0, 15 + 0, 18 + 0 and 21 + 0) from H9 hESCs were quantitated (n = 3). **E** Relative gene expressions of RUNX1, GATA1, FLI1, TAL1, KLF1, NFE2, PF4, β1-tubulin and FOG1 in suspension cells generated from cell spheroids from H9 hESCs at days 9, 12, 15, 18 and 21 were determined by RT-qPCR (n = 3). All data in B, D, E were represented as means ± SD. *$p < 0.05$, **$p < 0.01$, ***$p < 0.001$ and ns (no significance)

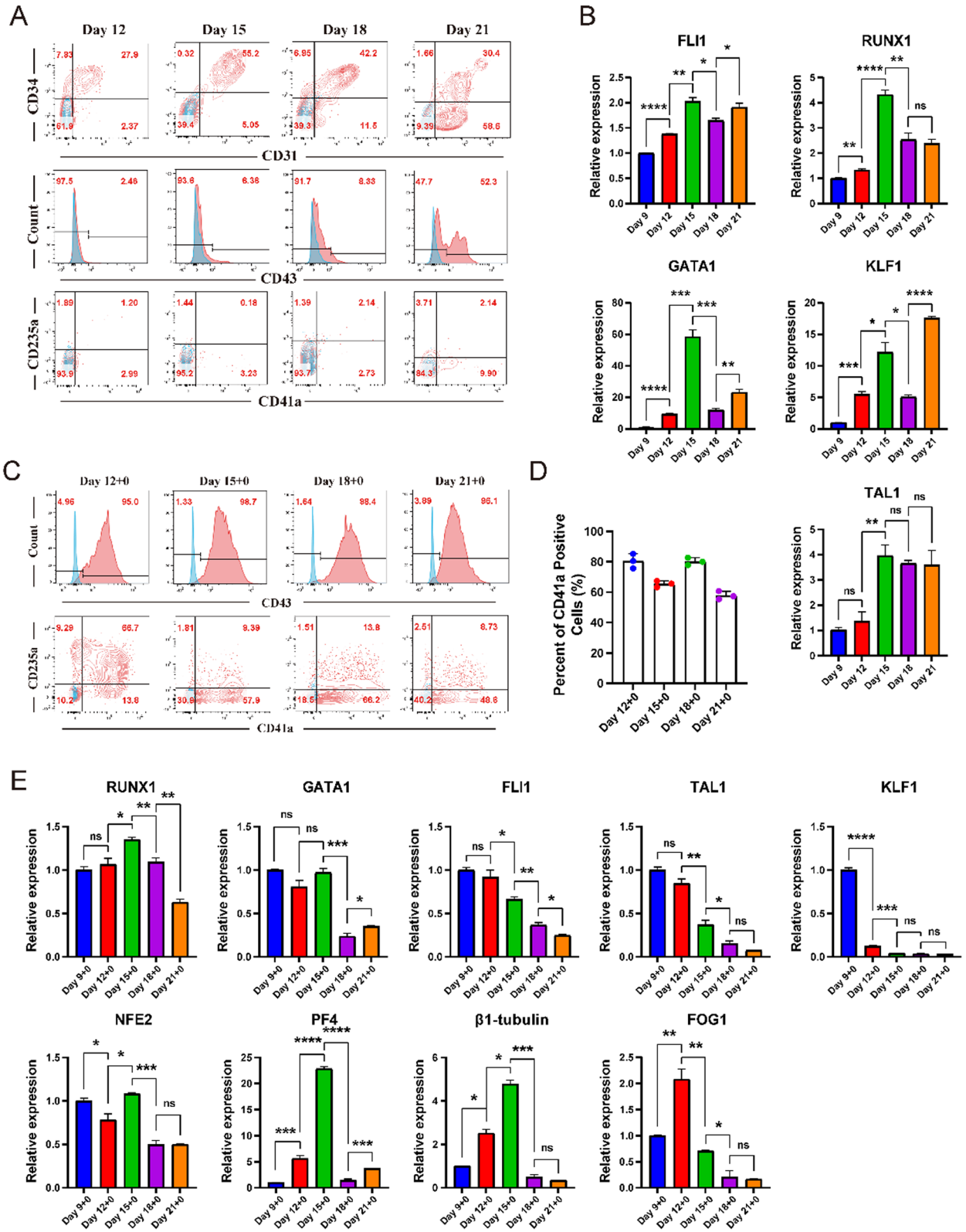

Fig. 4 (See legend on previous page.)

β1-tubulin) were expressed dynamically (Fig. 5H, Figure S13), and platelet-specific genes (FOG1, NFE1, PF4, ARNTL) were up-regulated (Fig. 5H, Figure S13), especially, ARNTL as a specific surface marker of platelet-producing MKs [32], in the derivatives of H1 and H9 cells, suggesting that MKs were maturated and prepared to produce platelets at the stage.

In order to further elucidate the differences among cells at days 9 (HEC spheroids), 9+0 (MEP suspension cells), 9+2 (early MKs) and 9+6 (mature MKs), whole-genome transcriptome analysis was conducted, and it revealed significant differences in their gene expression levels (Figure S14). Compared with the HEC spheroids at day 9, there were 4355 DEGs were down-regulated and 2284 DEGs (including TAL1, SELP and GFI1B, which were related to erythrocyte differentiation, platelet activation and MK differentiation, respectively) were up-regulated in MEP suspension cells at day 9+0 (Fig. 6A). We further identified 1255 up-regulated DEGs (including TREML1 and CD9, IL21R and SPP1, which were related to platelet activation and aggregation, as well as immune development) and 1917 down-regulated DEGs in cells at day 9+2 compared with those at day 9+0 (Fig. 6B). Moreover, 2322 DEGs (including GADD45B, CSF1 and CDKN2B, which were related to apoptosis, cytoskeleton reorganization and cell migration, and cell cycle regulation, respectively) were up-regulated and 1135 DEGs were down-regulated in cells at day 9+6 compared with those at day 9+2 (Fig. 6C). To explore the biological function of up-regulated DEGs, GO enrichment analysis was performed, and the results showed the enriched GO terms including DNA replication, mitotic nuclear division, myeloid cell differentiation, erythrocyte differentiation and MK differentiation at day 9+0 (Fig. 6D), and blood coagulation, platelet activation and platelet aggregation at day 9+2 (Fig. 6E), and regulation of immune effector process, regulation of coagulation and regulation of apoptotic signaling pathway at day 9+6, separately (Fig. 6F). In conclusion, these results indicated that hESC-derived MEPs could be differentiated into early MKs and then maturated into mature MKs in vitro.

Characterization and functional validation of platelets in vitro and in vivo

Since the cells at day 9+6 showed the characteristics of mature MKs with the potential to produce platelets, thus, MKs at day 9+6 were collected and subjected to induce platelet production (Fig. 7A). CD61 is a specific marker that serves both as a surface marker for MKs and as a surface marker for activation-dependent platelets [16]. In our in vitro differentiation system, there was 72.1% of platelets expressed CD61 at day 9+6, then the percentages were increased to over 96% or 93% after 8 more days' induction in the derivatives of both H9 cells and H1 cells (Fig. 7B, Figure S15A), similar to that of donor platelets (Figure S16A). To further distinguish functional platelets from the heterogeneity in vitro-produced pool, we collected platelets at day 9+14 to detect the expression level of CD62P and the binding ability of platelets to PAC-1 under the stimulation with ADP and TRAP-6. The results showed that after the stimulation, $CD62P^+$ platelets were significantly increased from 0.68% or 2.06% to 96.5% or 86.7%, and the ability to bind to PAC-1 was also increased significantly from 0.69% or 5.31% to 51.2% or 57% respectively with ADP/TRAP-6 in the derivatives of both H9 cells and H1 cells (Fig. 7C, Figure S15B), as was the case with donor platelets (Figure S16B), indicating that hESC-derived platelets had function in vitro. Thus, the above results provided the strong evidence on the development of functional platelets in vitro, supporting our differentiation approach recapitulated the in vivo development of MKs and platelets.

The major function of platelets is to guarantee primary hemostasis, followed by participating in the clotting process to contribute to the secondary process of hemostasis. Therefore, in order to evaluate the coagulation and hemostatic function of hESC-derived platelets in vivo, we developed a mouse model of thrombocytopenia, thus, the in vivo hemostatic function of hESC-derived platelets could be evaluated by measuring tail bleeding and the

(See figure on next page.)

Fig. 5 Characterization of hESC-derived MKs. **A** Schematic representation of MEPs developing into mature MKs. **B** Flow cytometric analysis for the percentages of CD41a and CD235a in suspension cells from H9 hESCs at days 9+0, 9+2, 9+4 and 9+6 (n=3). **C** The percentages of $CD41a^+$ cells in the hematopoietic suspension cells from H9 hESCs at days 9+0, 9+2, 9+4 and 9+6 were quantitated (n=3). **D** Flow cytometric analysis for the percentages of $CD41a^+CD42a^+$ cells, $CD41a^+CD42b^+$ cells from H9 hESCs at days 9+0, 9+2, 9+4 and 9+6. **E** Detection of polyploidy of suspension cells from H9 hESCs at day 9+6 by flow cytometry. **F** Giemsa staining was performed at day 9+6 after the differentiation of H9 hESCs. (Original magnification, 100x, Scale bar, 100 μm). **G** Co-immunofluorescent staining for CD62P and α-tubulin at day 9+6 after the differentiation of H9 hESCs. The colors of green, red and blue represented the staining for CD62P, α-tubulin, and nuclei, respectively. (Original magnification, 40x, Scale bar, 100 μm). **H** The relative expression levels of CD41a, CD42a, CD42b, CD62p, RUNX1, FLI1, GATA1, β1-tubulin, FOG1, NFE2, PF4 and ARNTL1 in H9 hESCs, cell spheroids at day 9, and the suspension cells from day 9+0 to day 9+6, as well as CB $CD34^+$ cell-derived MKs (CB-MKs) by RT-qPCR (n=3). All data in B, C, H were represented as means ± SD. *$p<0.05$, **$p<0.01$, ***$p<0.001$ and ns (no significance)

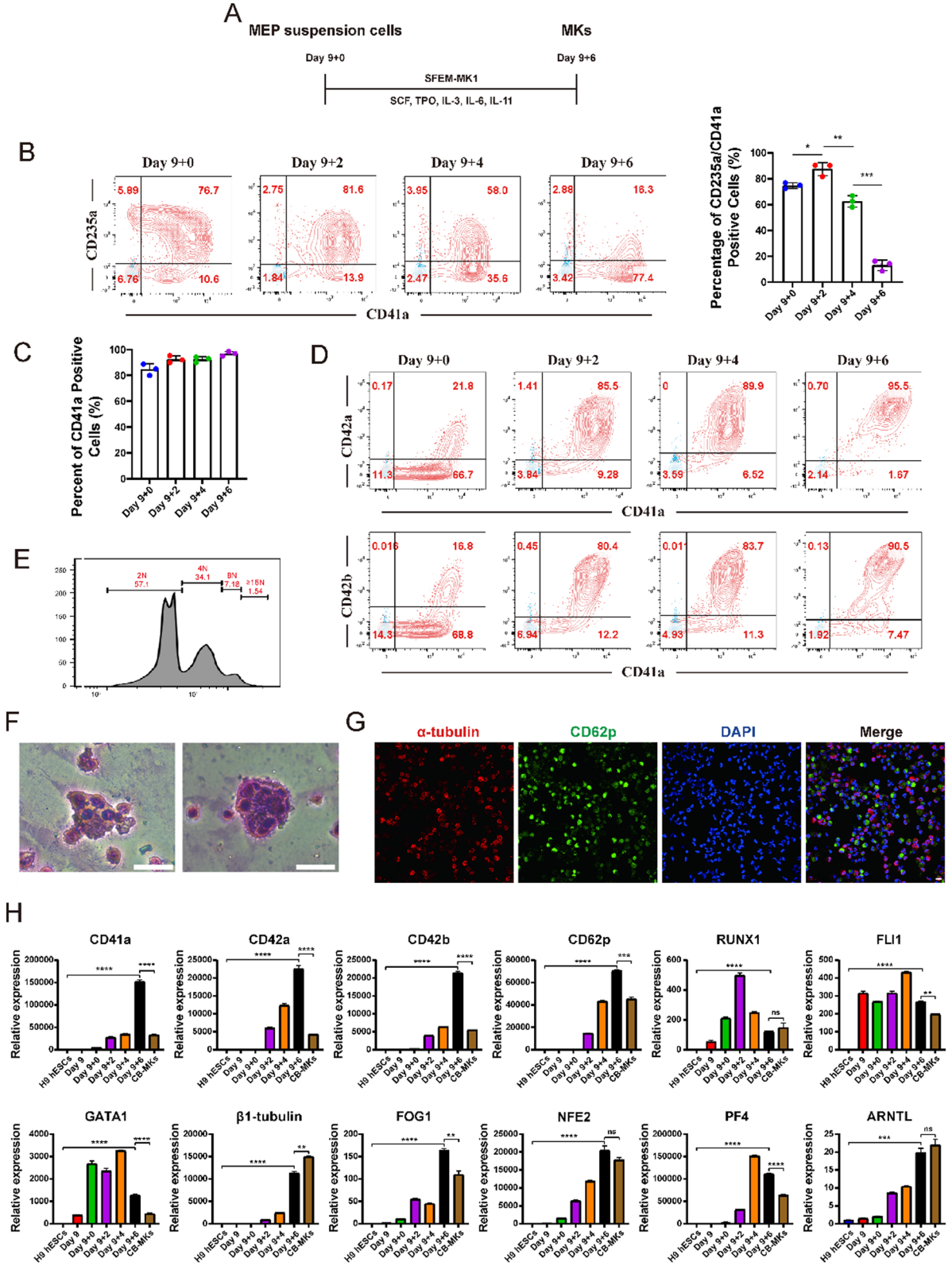

Fig. 5 (See legend on previous page.)

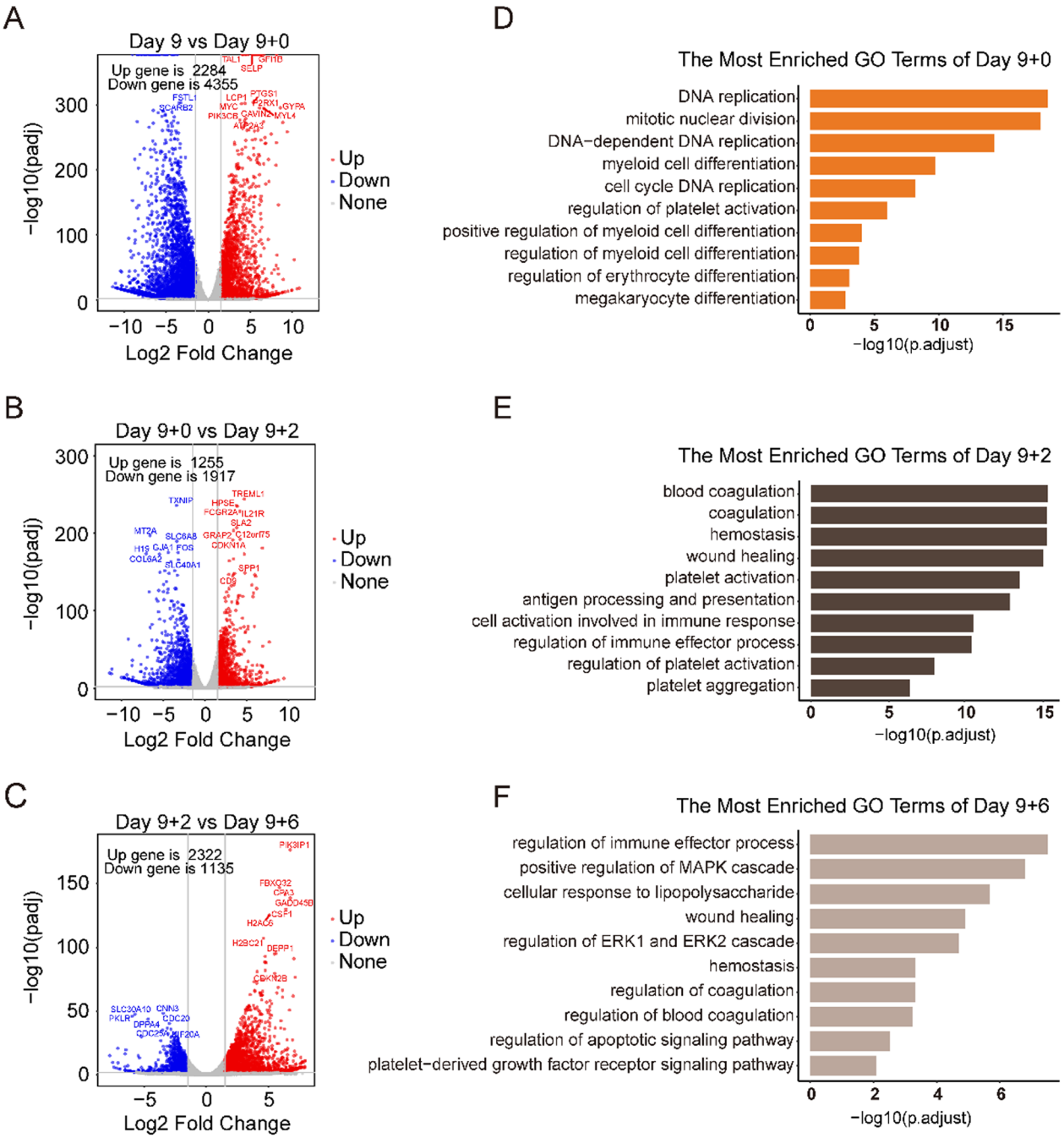

Fig. 6 Analysis of gene expression patterns for the differentiation of MEPs into mature MKs by transcriptional sequencing. **A**–**C** Volcano maps of DEGs between cells from H9 hESCs at day 9 + 0 and day 9 (**A**), day 9 + 2 and day 9 + 0 (**B**), day 9 + 6 and day 9 + 2 (**C**). Red spots represented up-regulated genes, blue spots represented down-regulated genes, and gray spots represented non-DEGs. (D-F) GO terms of up-regulated DEGs between cells from H9 hESCs at day 9 + 0 and day 9 (**D**), day 9 + 2 and day 9 + 0 (**E**), day 9 + 6 and day 9 + 2 (**F**)

involvement in secondary hemostatic process through measuring coagulation reactions by rescuing thrombocytopenia model. First of all, mice were injected with cyclophosphamide (CTX) for 3 consecutive days to consume platelets to establish a model of thrombocytopenia, and the weight of mice was recorded for 7 consecutive days. As the results shown in Fig. 7D, the weight of normal mice without treatment and mice injected with HBSS gradually increased. In contrast, mice injected with CTX gradually lost weight within 3 days after the injection and

reached their lowest weight at day 4. The mice began to re-gain weight when the administration of CTX was terminated. After three days of the induction with CTX, the platelet contents of the mice were significantly reduced before the treatment with injecting human platelets, indicating the successful establishment of the thrombocytopenia model (Fig. 7E). At the fourth day of modeling, we examined the coagulation and hemostatic function of mice. When compared with the normal mice without treatment by CTX and the mice injected with HBSS, the clothing time and the bleeding time of the model mice was significantly prolonged and the coagulation efficiency was significantly decreased using both slide and capillary approaches (Fig. 7F).

Next, mice were injected with hESC-derived platelets or human donor-derived platelets using the same dose at the fourth day of modeling, and blood samples were collected at 0.5, 1, 2, 4, 6, 24 and 48 h to detect the changes in the content of exogenous platelets in mice after the injections with human platelets or HBSS. After rescuing the model mice with the same dose of hESC-derived platelets or donor-derived platelets, the platelet contents of the mice were significantly recovered (Fig. 7E), and the kinetic process in vivo of the differentiated platelets was very similar to donor-derived platelets (Fig. 7G). Afterwards thrombocytopenia model mice were tested for coagulation and hemostatic function 4 h after injection. As shown in Fig. 7H, when compared with the model mice treated with HBSS, the blood coagulation time of mice injected with hESC-derived platelets or human donor-derived natural platelets was significantly shorter, and the rescue effect of human platelets from the two sources on the process of the blood coagulation efficiency and hemostasis in model mice was highly similar, indicating the coagulation and hemostatic function in model mice was significantly improved by human platelets (Fig. 7H). The coagulation efficiency of hESC-derived platelets was further evaluated by comparing the bleeding time, and the results showed that the hemostatic efficiency of model mice was significantly improved after the treatment with two kinds of exogenous platelets, and the hemostatic effects of the two kinds of platelets were also similar, even showing no significant difference when compared to those of normal mice (Fig. 7I). Together, these results strongly demonstrated that hESC-derived platelets had similar in vivo coagulation and hemostatic functions as human donor-derived platelets did, exhibiting in vivo function by improving the coagulation and hemostasis in thrombocytopenia mice.

Mechanism by which hESCs were differentiated into mature MKs in vitro

To further validate the differentiation approach, transcriptome sequencing was performed to reveal the expression profiles of cells at day 0 (H9 cells), 2, 6, 9, 9+0, 9+2 and 9+6 during the differentiation. To obtain an overview of the differences of the gene expression among different cells at various stages of the megakaryopoiesis, we first performed correlation analysis and principal component analysis (PCA) model to realize the visual representation. The results showed that these samples clustered by their biological replicates and the expression level of the genes among most of the groupings was significantly different (Fig. 8A–B). However, it also showed the similarities between cells at day 2 and H9 cells (day 0), at day 6 and day 9, and among cells at day 9+0, day 9+2 and day 9+6 cells (Fig. 8A).

Subsequently, to more intuitively show the differential genes upon the differentiation, specific genes at different differentiation stages were selected for analysis. Specifically, we found that stage-related genes at each stage were significantly highly expressed. Briefly, transcripts associated with pluripotency such as SOX2 and NANOG were highly expressed in hESCs and rapidly downregulated during the megakaryopoiesis (Fig. 8C). In contrast, genes associated with primitive mesoderm formation such as

(See figure on next page.)

Fig. 7 Characterization of platelet function in vitro and in vivo. **A** A schematic representation of platelets differentiated from hESC-derived MKs. **B** Flow cytometry analysis for CD61 expression of H9 hESC-derived platelets. **C** Flow cytometry analysis for PAC-1 binding, P-selectin and CD42b expression of H9 hESC-derived platelets with or without 100 μM ADP and 40 μM TRAP-6 together. **D** Dynamic changes of body weights of mice treated with cyclophosphamide (CTX), HBSS or without the treatment (Normal-untreated) respectively for 7 days (n = 4). **E** Changes in the number of platelets in mice at each group, including before modeling with cyclophosphamide (Pre-CTX), before the treatment with platelets or HBSS after modeling (Pre-injection), 0.5 h and 4 h after the treatment with HBSS or platelets (Injection 0.5 h, Injection 4 h) (n = 4). **F** Clotting times and bleeding times of thrombocytopenia model mice and normal mice on the fourth day of developing the model (n = 4). Normal-untreated: normal healthy mice were used as blank control; HBSS: mice induced by HBSS (solvent of cyclophosphamide) that did not acquire thrombocytopenia; CTX: cyclophosphamide-induced thrombocytopenia model mice. **G** Proportions of human donor-derived platelets or H9 hESC-derived platelets in thrombocytopenia model mice were detected by flow cytometry at 0.5, 1, 2, 4, 6, 24 and 48 h after the treatment with human platelets (n = 4). **H**, **I** Clotting times (**H**) and bleeding times (I) of thrombocytopenia model mice and normal mice on the fourth day of developing the model after the treatment with platelets (n = 4). CTX mice + HBSS: injection of HBSS to treat thrombocytopenia model mice, as placebo group; CTX mice + hESC-Platelet: injection of hESC-derived platelets to treat thrombocytopenia model mice; CTX mice + Donor-Platelet: injection of Donor-derived platelets to treat thrombocytopenia model mice; Normal-untreated: normal healthy mice, as a control

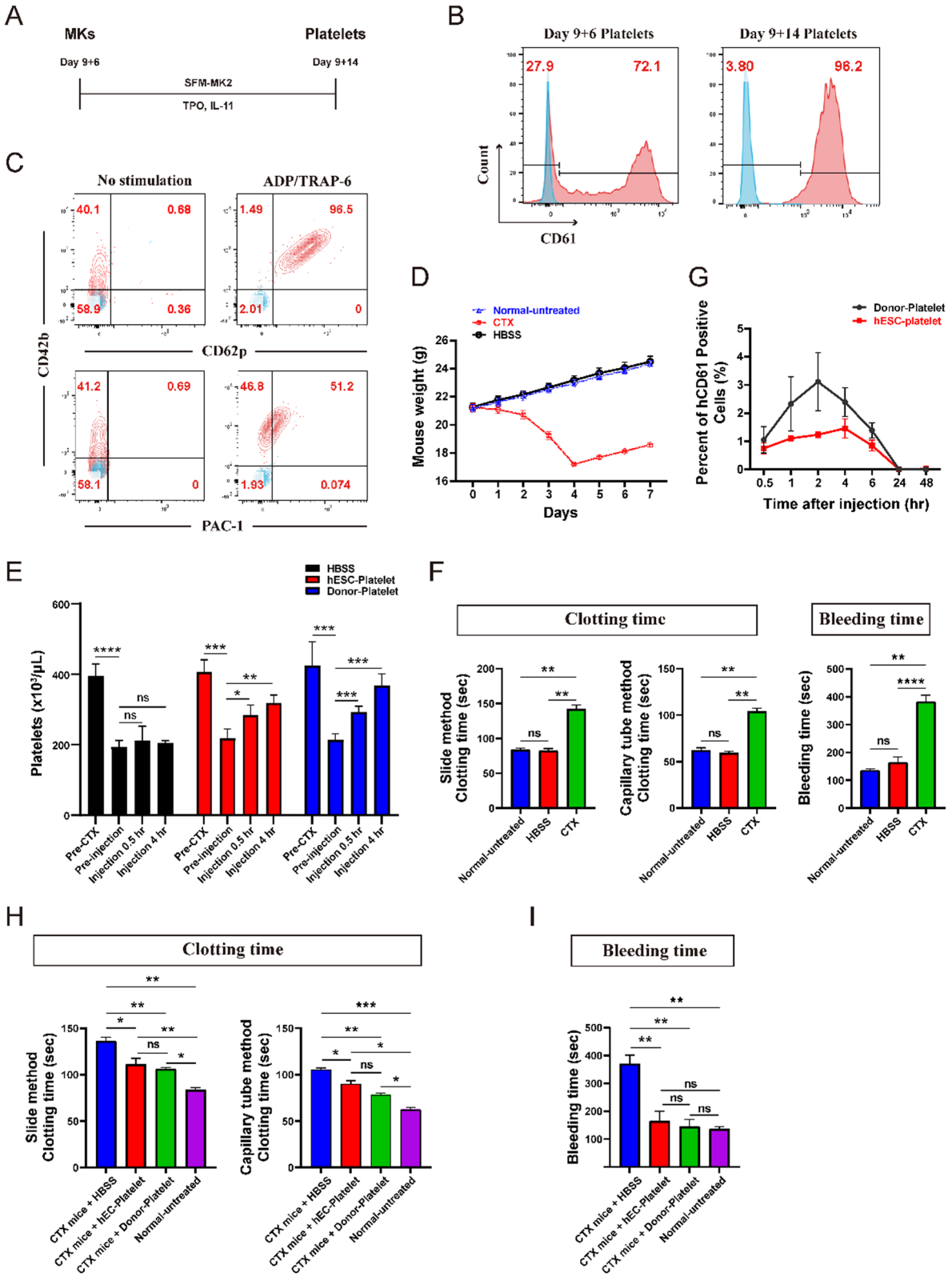

Fig. 7 (See legend on previous page.)

SP5, FST and TBXT were highly enriched in MPCs at day 2 (Fig. 8C). At day 6, cells began to gradually express endothelium and arterial endothelium related genes, including vWF, CD44, GJA5, HOXB5, HOXA10, CD34, VCAM, KGR in early HECs (Fig. 8C). Human endothelial cells of arterial origin was found to show the great potential to develop into hematopoietic endothelium in comparison with endothelial cells of venous origin, suggesting that the differences in endothelial surfaces contribute to identify their hematopoietic potential [36]. Consistent with aforementioned analysis of Go terms, cells at this stage were significantly enriched in the biological processes of endothelial development and the angiogenesis (Fig. 1H). Subsequent cell spheroids at day 9 showed high characteristic expression of hematopoietic endothelial and early hematopoiesis related genes, including CDH5, ERG and MECOM in late HECs (Fig. 8C). Therefore, the above results indicated that the cell spheroids at day 6 had been developed into the endothelial stage and gradually entered hematopoietic endothelial stage, which was then transformed into hematopoietic cells, and this process was further strengthened at day 9. Interestingly, we found the gene expression patterns of MEP suspended cells from HEC spheroids (at day 9 + 0) were significantly changed when compared to those of HEC spheroids (at day 9) (Figs. 8A–C and 6A–C). The cells in HEC spheroids mainly expressed characteristic genes related to hematopoietic endothelium and early hematopoiesis mentioned above, while megakaryocytic-erythroid lineage genes such as GYPA and KLF1 were highly expressed in MEPs (Fig. 8C). Collectively, these results indicated that the suspended cells at day 9 + 0 might be defined as MEPs. And the flow cytometry analysis results also provided strong supporting evidence for this conclusion (Fig. 5B, C). After further induction for MKs, the expression levels of MK-specific genes such as RUNX1, MPL, FLI1 and ZFPM1 were gradually increased, while on the other hand, the expression of erythroid-related genes such as GYPA and KLF1 was dramatically decreased in early MKs at day 9 + 2 (Fig. 8C). Together, these data suggested that hESC-derived MEPs gradually developed towards MKs during this step. Finally, GP1BA, GP1BB, PF4, NFE2, PTPRC, SLEP and CD9, which are related to mature MKs and platelet activation as well as platelet adhesion, were highly expressed mature MKs at day 9 + 6 (Fig. 8C). Therefore, it appeared that cells after day 9 + 2 gradually developed into mature MKs, and began to possess the capacity to produce platelets at day 9 + 6.

To explore the signaling pathways which play a vital role during the megakaryopoiesis, GO and Encyclopedia of Genes and Genomes (KEGG) enrichment analysis were performed. The KEGG pathway analysis revealed that the differentially expressed mesoderm genes were correlated to the pluripotency of stem cells and Wnt signaling pathway at day 2 (Fig. 8D). Among them, Wnt signaling pathway is the most investigated and the best characterized as a key pathway in mesoderm development [37], thus indicating here a close transition from hESCs to MPCs (Fig. 1F). Spheroids at day 6 were developed into HECs with the potential to generate early hematopoietic cells (Fig. 1B–C, Fig. 8C). At this stage, we found that HEC spheroids at day 6 were significantly enriched in Apelin signaling pathway and Vascular smooth muscle contraction related to endothelial development [38, 39], and in PI3K-Akt signaling pathway and MAPK signaling pathway related to cell proliferation (Fig. 8D) [40, 41]. It appeared that Apelin signaling pathway and Vascular smooth muscle contraction mediated the differentiation of mesodermal cells into endothelial cells at this stage, and PI3K-Akt and MAPK signaling pathways promoted the proliferation of endothelial cells formed at this stage. On days from 6 to 9, early hematopoietic cells were gradually developed into MEPs which shed from HEC spheroids to the culture medium. KEGG analysis revealed that this process might be facilitated by the synergistic effect of three upregulated signaling pathways including neuroactive ligand-receptor interaction, calcium signaling pathway and cAMP signaling pathway (Fig. 8D), and it was likely that these three pathways acted in concert to promote the shedding of individual MEP suspension cells from the HEC spheroids. Interestingly, MEP suspension cells at this stage (day 9 + 0) were predominantly enriched in signaling pathways associated with cell proliferation, including DNA replication and cell cycle in KEGG enrichment analysis (Fig. 8E), similar to the results of GO (Fig. 6E), suggesting that this stage was a period of rapid

(See figure on next page.)

Fig. 8 Transcriptome analysis for the mechanism of the differentiation of hESCs into mature MKs in vitro. **A** Heatmap of correlation and PCA analyses of H9 hESCs, differentiated cells at days 2, 6, 9, 9 + 0, 9 + 2 and 9 + 6. **B** Principal component analysis (PCA) of H9 hESCs, differentiated cells at days 2, 6, 9, 9 + 0, 9 + 2 and 9 + 6. **C** Expression analysis of specific high-expressing genes at different stages during H9 hESC-derived megakaryopoiesis. **D**, **E** KEGG enrichment analysis of up-regulated genes (H9 hESCs vs cells at day 2, cells at day 2 vs cells at day 6, cells at day 6 vs cells at day 9, cells at day 9 vs cells at day 9 + 0, cells at day 9 + 0 vs cells at day 9 + 2, cells at day 9 + 2 vs cells at day 9 + 6). (**F**–**H**) PPI network of up-regulated DEGs between cells from H9 hESCs at day 9 + 0 and day 9 (F), day 9 + 2 and day 9 + 0 (G), day 9 + 6 and day 9 + 2 (H) analyzed in STRING database. The rank is in descending order from red to yellow

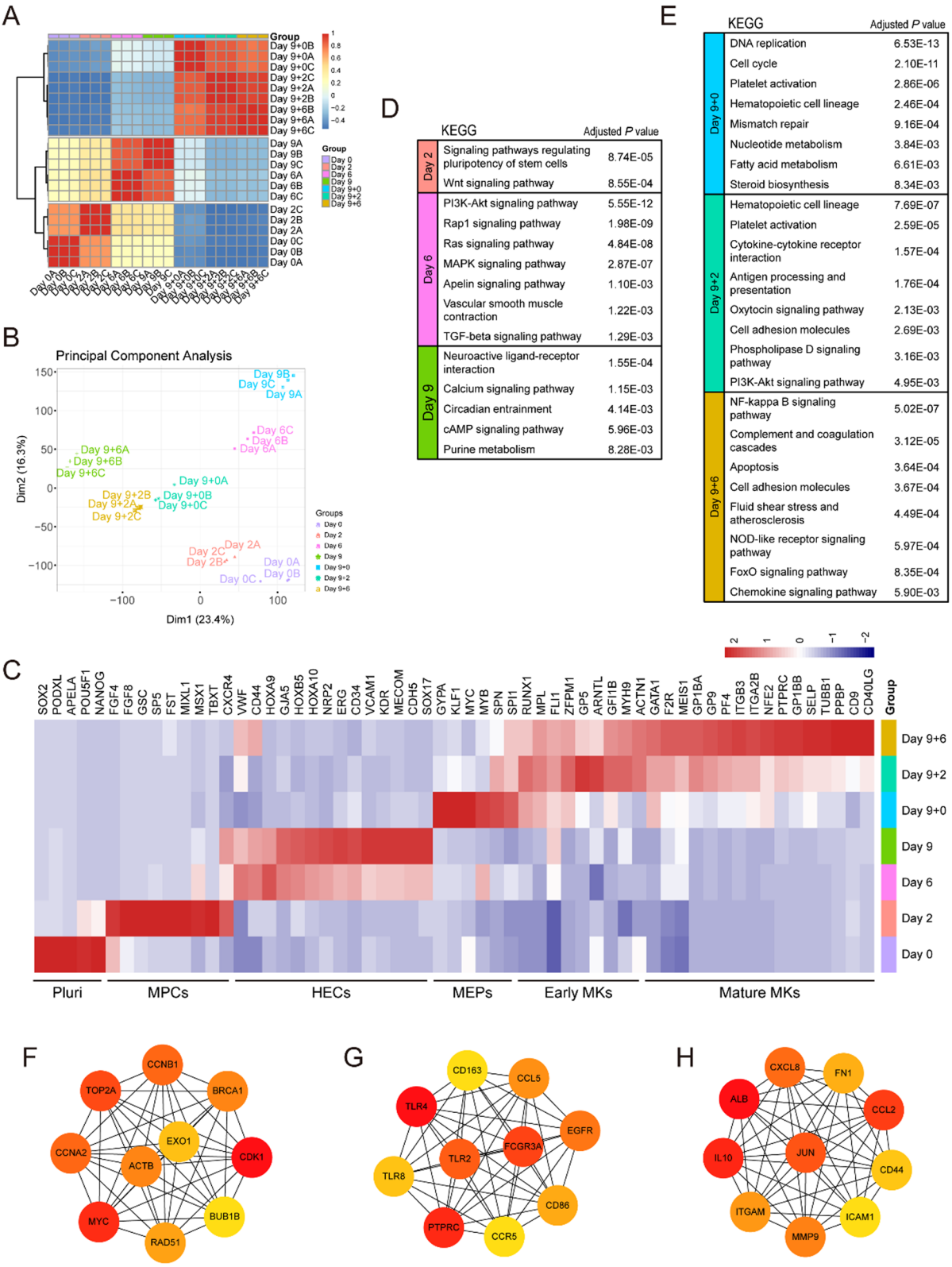

Fig. 8 (See legend on previous page.)

proliferations of MEPs and early MKs. MKs at day 9+2 were undergoing a rapid maturation phase (Fig. 5D), and KEGG enrichment analysis showed that these cells at this stage significantly expressed oxytocin signaling pathway, phospholipase D signaling pathway and PI3K-Akt signaling pathway (Fig. 8E), these results suggested that these three signaling pathway contributed to promote the maturation of MKs. Moreover, KEGG was conducted to reveal that MKs at day 9+6 enriched signaling pathways related to apoptosis, complement and coagulation cascades as well as fluid shear stress and atherosclerosis (Fig. 8E), which played vital roles in promoting that MKs finally were matured and began to possess the capacity to produce platelets.

In addition, we focused on what genes might play important roles during the induction phase of MKs. We analyzed PPI network of differentially expressed genes in cells at different induction stages in STRING database and screened for potential proteins that regulate MK differentiation, maturation, and platelet production (Fig. 8F–H). The results of PPI analysis showed that genes such as CDK1, MYC, and TOP2A were closely linked at day 9+0 of the induction, and were Hub Genes (Highly Connected Genes). It has been shown that CDK1 plays a role in the regulation of the mitosis during MK differentiation [42]; MYC, as a regulator of cell growth, proliferation and differentiation, promotes NK proliferation by facilitating cell growth and polyploidization while transiently inhibiting cell differentiation (Fig. 8C) [43]; at the same time, TOP2A participates in the early process of development and cell proliferation through synergistic action. In parallel, TOP2A is involved in cell proliferation during the early development and regulates MK proliferation through synergistic effects with other key genes [44]. At day 9+2 of the induction, PPI analysis showed that TLR4 and EGFR were closely linked as Hub Genes at this stage. It has been shown that TLR4 plays an important role in the differentiation of hematopoietic progenitor cells, especially affecting myeloid differentiation [45]. Not only that, but its co-stimulation with other TLRs affects MK development [46]. The activation of EGFR leads to the downstream signaling involving PI3 kinase-dependent AKT phosphorylation and Ca^{2+} transients, which are critical for platelet function [47]. VEGFR-1 enhances MK maturation and increases platelet production [48, 49]. Since EGFR and VEGFR signaling pathways can interfere with each other, it was hypothesized that EGFR might regulate MK maturation by affecting VEGFR signaling. At day 9+6 of the induction, PPI analysis showed that genes such as ALB and JUN were closely linked and were Hub Genes at this stage. It has been shown that ALB has a significant effect on platelet generation and function, and that ALB can regulate platelet adhesion through its conformational state [50, 51]; JUN is a positive regulator of cell proliferation and differentiation [52], which contributes to MK maturation and platelet biogenesis by promoting DNA synthesis and polyploidization [53].

Discussion

Here, we developed a novel, stepwise, completely xeno-free, defined three-dimensional culture system to robustly generate MKs and platelets from hESCs by rigorously modeling the development of MKs and platelets in vivo. In this system, hESCs were successfully induced sequentially into MPC spheroids and HEC spheroids, where HEC spheroids could generate early hematopoietic cells, and these early hematopoietic cells could develop into MEP suspension cells. Individual MEP suspension cells isolated from these spheroids were then induced and stimulated by different combinations of cytokines to differentiate into MK lineage and further developed into mature MKs, which ultimately gave rise to functional platelets. hESC-derived MKs could reach a purity level over more than 95%, and they possessed characteristics of mature MKs, such as the expression of CD42a and CD42b, the formation of multinucleated structures, and the presence of more than 8N DNA, which could be used for the development of MEPs and MKs. Moreover, in vivo functionality of hESC-derived platelets was also documented in thrombocytopenia mice by evaluating the thrombus formation in vivo and the haemostasis, showing a similar blood coagulation time and hemostatic efficiency when compared with human natural platelets. Thus, hESC-derived platelets exhibited in vivo function at the improvement of the coagulation and hemostasis, which was similar to that of the donor-derived platelets.

Transcriptome sequencing is an effective method to reveal gene expression profiles and explore important regulatory pathways during the differentiation. To further investigate the transcriptional changes of genes during the differentiation, we analyzed their gene expression and correlation between undifferentiated and various-differentiated states during the megakaryopoiesis under our differentiation system. Multiple signaling pathways, including Wnt and TGF-β signaling pathways, were reported to be associated with the generation and function of MKs. Consistent with the previous studies [28, 29, 36, 54], our results indicated that Wnt signaling dominantly regulated the development of hESCs to the mesoderm stage (Fig. 6C), and our results also showed that TGF-β signaling pathway played an important role in the development of mesoderm to hematopoietic endothelium stage (Fig. 6C). Furthermore, various metabolic pathways began to up-regulate, such as purine metabolism, nucleotide metabolism and fat metabolism, during the stage of endothelial to hematopoietic transition

(EHT). Then we further confirmed that short-term induction of TPO with other cytokines significantly improved the differentiation of early hematopoietic cells into MEPs, along with the upregulation of the signaling pathways such as DNA replication and cell cycle. Subsequently those MEPs proliferated rapidly and favored the development of MK lineage at this phase. Taken together, these findings demonstrated that short-term induction of TPO impaired erythroid differentiation capacity and promoted megakaryocytic differentiation of MK/erythroid progenitors. After further development into more mature MKs, signaling pathways such as phospholipase D signaling and PI3K-Ark signaling pathing were at high expression, and platelet activation signaling pathway begin to be enriched. At this time, immune-related signaling pathways, such as Antigen processing and presentation, were also up-regulated to a certain extent in hESC-derived MKs.

Upon hESC-derived MKs further maturating into polyploid mature MKs and entering an apoptotic stage, we observed that platelet-related signaling pathways, such as Complement and Cascades and Fluid shear stress and atherosclerosis, were gradually activated. MKs developed in vivo are heterogeneous, including various MKs which respectively regulate HSC maintenance, immune response, and platelet production. Consistent with others [32], in our in vitro differentiation system, signaling pathways related to immunity and inflammation were significantly enriched from day 9 + 2, which might be established by highly mimicking the in vivo differentiation process of MKs, and thus inevitably produced some MKs with immune characteristics. Therefore, it also likely be a reason for the low platelet production from hESC-derived MKs in vitro. Therefore, our study represents a significant advancement in the fields of stem cell-based hematopoiesis including the megakaryopoiesis and thrombopoiesis, regenerative medicine. Further studies would focus on elucidating the molecular mechanisms that mediate the formation and function of subpopulation of platelet-producing MKs, which might help circumvent future bottlenecks in platelet yields for clinical application.

hPSCs play a key role in regenerative medicine, and they can serve as a potential alternative source for a wide range of cells. In this study, hESCs were selected, mainly due to in view of the fact that hESCs are widely accepted in regenerative medicine and clinical applications. In addition, hESCs have relatively low immunogenicity, especially in allografts, which may reduce the risk of the rejection [55]. Human iPSCs can be obtained from patient's autologous cells with low immune responses, avoiding ethical considerations, however, their reprogramming process may introduce genetic mutations or instability, which may raise the concern on the safety of the cells in clinical application. Therefore, hESCs show some advantages in clinical applications.

Recently, immortalized MK progenitor cell lines (imMKCLs) were derived from human iPSCs through the transduction with BMI1, c-MYC, and BCL-XL or by co-culture with stromal cells [10, 56]. In addition, major advancements have been achieved in generating MKs from a variety of different stem cell sources and the development of platelet bioreactor systems [21, 56–58], however, the introduction of exogenous genes or heterologous cells remain suboptimal for clinical use, with limitations mainly related to immune rejection, genetic instability, and the complexity of clinical translation. Exogenous genes may lead to abnormal cell function and cancer risk, while heterologous cells are easily recognized and rejected by host immune system after the transplantation. In addition, the high cost of culture and production increase the economic burden of clinical application. At the same time, the integration and implementation of these technologies are complex and requires strict regulatory and ethical scrutiny, further reducing the feasibility of their translation into actual therapies. Thus, these factors together may hinder their widespread application in regenerative medicine.

Since our established hESC-derived platelet system is compositionally defined and heterologous-free, it holds great potential for clinical application. However, further improvement of the purity and yield of platelets, as well as further reduction of potential immunogenicity issues, are needed for hESC-derived platelets generated by the present system to clinical applications. As the current differentiation system was developed by mimicing the developmental process of MKs and platelets in vivo, the generation of MKs is likely to be heterogeneous, and different MK subpopulations have significant differences in their abilities to produce platelets; at the same time, our culture system could not fully mimic bone marrow microenvironment, thus, immature MKs might remain in the final product, affecting the purity and function of platelets. In addition, MK development and platelet production are regulated by a variety of signaling pathways, including MAPK, PI3K/Akt and NF-κB, and some of them are related to immune regulation, which may contribute to the release of immune factors to affect MK survival and platelet release, or even activate platelets prematurely. Thus, inappropriate activation of immune response-related signaling pathways may lead to potential safety issues with hESC-derived platelets, such as excessive activation that may cause unwanted coagulation, inflammatory responses, or immune responses. Therefore, targeted studies are needed in future research to address these challenges. For example, the use of

single-cell RNA sequencing to identify different subpopulations of MKs and their potential functions to improve the number of platelet-producing MKs, and the optimization of culture conditions to promote the efficient expansion of MKs; the development of culture systems that more closely mimic bone marrow microenvironment to further enhance the maturation of MKs and the efficient production of platelets with the functionality including their hemostatic function and survival rate in vivo.

Conclusions

In conclusion, we have developed a four-stage differentiation approach for the efficient generation of mature MKs and platelets under 3D differentiation conditions. The in vivo coagulation and hemostasis function of hESC-derived platelets were found to be similar to that of human donor-derived platelets, indicating a new emerging method for the preparation of functional platelets suitable for future clinical applications.

Abbreviations

hESCs	Human embryonic stem cells
MKs	Megakaryocytes
hPSCs	Human pluripotent stem cells
HSCs	Hematopoietic stem cells
HSPCs	Hematopoietic stem/progenitor cells
CLPs	Common lymphoid progenitors
CMPs	Common myeloid progenitors
MEPs	MK-erythrocyte progenitors
TPO	Thrombopoietin
MKPs	Megakaryocyte progenitors
MPC	Mesodermal progenitor cell
HEC	Hematopoietic endothelial cell
EHT	Endothelium-hematopoietic transformation
CTX	Cyclophosphamide

Supplementary Information

The online version contains supplementary material available at https://doi.org/10.1186/s13287-024-04071-x.

Additional file 1.

Acknowledgements

The authors declare that they have not used Artificial Intelligence in this study.

Author contributions

CXC, NW, XYZ and YJF designed the study. CXC and NW wrote the manuscript. CXC, NW, XYZ, YJF, ZYZ, and HBW performed the in vitro and in vivo experiments. YYD and YMW conceived and designed the experiments, and YYD and YMW provided financial support. All authors contributed to the manuscript and approved the submission.

Funding

This work was supported in part by the National Key Research and Development Program of China (2018YFA0108200, 2018YFA0108201, 2018YFA0108204), by Research Starting Funding of South China University of Technology (D6201880, K5180910, K5204120, and D6212440), by Research Starting Funding of the Second Affiliated Hospital of South China University of Technology (KY09060026), by Research Agreement between South China University of Technology and Guangzhou First People's Hospital (D9194290), by Key Clinical Technology Program of Guangzhou (2019ZD18).

Data availability

The data that support the findings of this study are available from the corresponding author upon reasonable request. The detail Methods and Materials were provided in Supplementary Information. RNA sequencing data have been uploaded to GEO database and are available with accession number GSE216593.

Declarations

Ethics approval and consent to participate

This study was approved by the Ethics Committee of Guangzhou First people's Hospital (Approval No.: K-2021–008-01, and approval date: January 17, 2022.) to use umbilical cord blood and human platelets from healthy volunteers for Large-scale Preparation of Functional Platelets from hESCs/iPSCs. The patients or their guardians/legally authorized representatives provided written informed consent for participation in the study with the use of umbilical cord blood and human platelets. All mouse experiments were performed according to our experimental protocols approved by the Guangzhou Committee for the Use and Care of Laboratory Animals, and by the Animal Ethics Committee of South China University of Technology University (Approval number: 2019073, and approval date: December 12, 2019.). WiCell Research Institute has confirmed that there was the ethical approval for collection of human embryonic stem cells (WA01(H1) and WA09(H9)) with NIH Approval NIHhESC-10–0043 and NIH Approval NIHhESC-10–0062, and that the donors had signed informed consent (www.wicell.org).

Competing interests

The authors declare that there is no competing interests.

Author details

[1]Laboratory of Stem Cells and Translational Medicine, Institute for Clinical Medicine, the Second Affiliation Hospital, School of Medicine, South China University of Technology, No.1 Panfu Road, Guangzhou 510180, People's Republic of China. [2]Laboratory of Stem Cells and Translational Medicine, Institutes for Life Sciences, School of Medicine, South China University of Technology, Guangzhou 510006, China. [3]Department of Blood Transfusion, the Second Affiliation Hospital, School of Medicine, South China University of Technology, No. 1 Panfu Road, Guangzhou 510180, China. [4]National Engineering Research Center for Tissue Restoration and Reconstruction, South China University of Technology, Guangzhou 510006, China. [5]The Innovation Centre of Ministry of Education for Development and Diseases, the Second Affiliated Hospital of South China University of Technology, School of Medicine, South China University of Technology, Guangzhou 510006, China.

Received: 5 August 2024 Accepted: 20 November 2024
Published online: 28 November 2024

References

1. Patel SR, Hartwig JH, Italiano JE Jr. The biogenesis of platelets from megakaryocyte proplatelets. J Clin Invest. 2005;115(12):3348–54.
2. Harrison P. Platelet function analysis. Blood Rev. 2005;19(2):111–23.
3. Versteeg HH, Heemskerk JW, Levi M, Reitsma PH. New fundamentals in hemostasis. Physiol Rev. 2013;93(1):327–58.
4. Vinholt PJ. The role of platelets in bleeding in patients with thrombocytopenia and hematological disease. Clin Chem Lab Med. 2019;57(12):1808–17.
5. Hill QA, Stamps R, Massey E, Grainger JD, Provan D, Hill A. The diagnosis and management of primary autoimmune haemolytic anaemia. Br J Haematol. 2017;176(3):395–411.
6. Deutsch VR, Tomer A. Megakaryocyte development and platelet production. Br J Haematol. 2006;134(5):453–66.
7. Margraf A, Nussbaum C, Sperandio M. Ontogeny of platelet function. Blood Adv. 2019;3(4):692–703.

8. Takayama N, Nishikii H, Usui J, Tsukui H, Sawaguchi A, Hiroyama T, et al. Generation of functional platelets from human embryonic stem cells *in vitro* via es-sacs, vegf-promoted structures that concentrate hematopoietic progenitors. Blood. 2008;111(11):5298–306.
9. Moreau T, Evans AL, Vasquez L, Tijssen MR, Yan Y, Trotter MW, et al. Large-scale production of megakaryocytes from human pluripotent stem cells by chemically defined forward programming. Nat Commun. 2016;7:11208.
10. Nakamura S, Takayama N, Hirata S, Seo H, Endo H, Ochi K, et al. Expandable megakaryocyte cell lines enable clinically applicable generation of platelets from human induced pluripotent stem cells. Cell Stem Cell. 2014;14(4):535–48.
11. Seita J, Weissman IL. Hematopoietic stem cell: Self-renewal versus differentiation. Wiley Interdiscip Rev Syst Biol Med. 2010;2(6):640–53.
12. Zhou Y, Zhu X, Dai Y, Xiong S, Wei C, Yu P, et al. Chemical cocktail induces hematopoietic reprogramming and expands hematopoietic stem/progenitor cells. Adv Sci (Weinh). 2020;7(1):1901785.
13. Thon JN, Italiano JE. Platelet formation. Semin Hematol. 2010;47(3):220–6.
14. Shen J, Zhu Y, Lyu C, Feng Z, Lyu S, Zhao Y, et al. Sequential cellular niches control the generation of enucleated erythrocytes from human pluripotent stem cells. Haematologica. 2020;105(2):e48–51.
15. Handtke S, Steil L, Palankar R, Conrad J, Cauhan S, Kraus L, et al. Role of platelet size revisited-function and protein composition of large and small platelets. Thromb Haemost. 2019;119(3):407–20.
16. Kauskot A, Hoylaerts MF. Platelet receptors. Handb Exp Pharmacol. 2012;210:23–57.
17. Liu C, Huang B, Wang H, Zhou J. The heterogeneity of megakaryocytes and platelets and implications for *ex vivo* platelet generation. Stem Cells Transl Med. 2021;10(12):1614–20.
18. Choudry FA, Bagger FO, Macaulay IC, Farrow S, Burden F, Kempster C, et al. Transcriptional characterization of human megakaryocyte polyploidization and lineage commitment. J Thromb Haemost. 2021;19(5):1236–49.
19. Du KL, Chen M, Li J, Lepore JJ, Mericko P, Parmacek MS. Megakaryoblastic leukemia factor-1 transduces cytoskeletal signals and induces smooth muscle cell differentiation from undifferentiated embryonic stem cells. J Biol Chem. 2004;279(17):17578–86.
20. Mazzi S, Lordier L, Debili N, Raslova H, Vainchenker W. Megakaryocyte and polyploidization. Exp Hematol. 2018;57:1–13.
21. Borst S, Sim X, Poncz M, French DL, Gadue P. Induced pluripotent stem cell-derived megakaryocytes and platelets for disease modeling and future clinical applications. Arterioscler Thromb Vasc Biol. 2017;37(11):2007–13.
22. Thon JN, Dykstra BJ, Beaulieu LM. Platelet bioreactor: accelerated evolution of design and manufacture. Platelets. 2017;28(5):472–7.
23. Karagiannis P, Eto K. Manipulating megakaryocytes to manufacture platelets *ex vivo*. J Thromb Haemost. 2015;13(Suppl 1):S47-53.
24. Wang N, Chen C, Cheng Y, Fu Y, Zhong Z, Yang Y, et al. Hypoxia drives hematopoiesis with the enhancement of t lineage through eliciting arterial specification of hematopoietic endothelial progenitors from hesc. Stem Cell Res Ther. 2022;13(1):282.
25. Hawkins KE, Sharp TV, McKay TR. The role of hypoxia in stem cell potency and differentiation. Regen Med. 2013;8(6):771–82.
26. Ferretti E, Hadjantonakis AK. Mesoderm specification and diversification: From single cells to emergent tissues. Curr Opin Cell Biol. 2019;61:110–6.
27. Vodyanik MA, Thomson JA, Slukvin II. Leukosialin (cd43) defines hematopoietic progenitors in human embryonic stem cell differentiation cultures. Blood. 2006;108(6):2095–105.
28. Bai H, Xie YL, Gao YX, Cheng T, Wang ZZ. The balance of positive and negative effects of TGF-β signaling regulates the development of hematopoietic and endothelial progenitors in human pluripotent stem cells. Stem Cells Dev. 2013;22(20):2765–76.
29. Xie Y, Bai H, Liu Y, Hoyle DL, Cheng T, Wang ZZ. Cooperative effect of erythropoietin and TGF-β inhibition on erythroid development in human pluripotent stem cells. J Cell Biochem. 2015;116(12):2735–43.
30. Challen GA, Boles NC, Chambers SM, Goodell MA. Distinct hematopoietic stem cell subtypes are differentially regulated by TGF-beta1. Cell Stem Cell. 2010;6(3):265–78.
31. Raghuwanshi S, Dahariya S, Sharma DS, Kovuru N, Sahu I, Gutti RK. Runx1 and TGF-β signaling cross talk regulates ca(2+) ion channels expression and activity during megakaryocyte development. Febs j. 2020;287(24):5411–38.
32. Wang H, He J, Xu C, Chen X, Yang H, Shi S, et al. Decoding human megakaryocyte development. Cell Stem Cell. 2021;28(3):535-49.e8.
33. Fan X, Krzyzanski W, Wong RSM, Yan X. Fate determination role of erythropoietin and romiplostim in the lineage commitment of hematopoietic progenitors. J Pharmacol Exp Ther. 2022;382(1):31–43.
34. Dalby A, Ballester-Beltrán J, Lincetto C, Mueller A, Foad N, Evans A, et al. Transcription factor levels after forward programming of human pluripotent stem cells with GATA1, FLI1, and TAL1 determine megakaryocyte versus erythroid cell fate decision. Stem Cell Reports. 2018;11(6):1462–78.
35. Furie B, Furie BC. Mechanisms of thrombus formation. N Engl J Med. 2008;359(9):938–49.
36. Sturgeon CM, Ditadi A, Awong G, Kennedy M, Keller G. Wnt signaling controls the specification of definitive and primitive hematopoiesis from human pluripotent stem cells. Nat Biotechnol. 2014;32(6):554–61.
37. Zeng Y, He J, Bai Z, Li Z, Gong Y, Liu C, et al. Tracing the first hematopoietic stem cell generation in human embryo by single-cell RNA sequencing. Cell Res. 2019;29(11):881–94.
38. Helker CS, Eberlein J, Wilhelm K, Sugino T, Malchow J, Schuermann A, et al. Apelin signaling drives vascular endothelial cells toward a pro-angiogenic state. Elife. 2020;9:e55589.
39. Kang Y, Kim J, Anderson JP, Wu J, Gleim SR, Kundu RK, et al. Apelin-apj signaling is a critical regulator of endothelial mef2 activation in cardiovascular development. Circ Res. 2013;113(1):22–31.
40. Sun Y, Liu WZ, Liu T, Feng X, Yang N, Zhou HF. Signaling pathway of mapk/erk in cell proliferation, differentiation, migration, senescence and apoptosis. J Recept Signal Transduct Res. 2015;35(6):600–4.
41. Wei D, Rui B, Qingquan F, Chen C, Ping HY, Xiaoling S, et al. Kif11 promotes cell proliferation via erbb2/pi3k/akt signaling pathway in gallbladder cancer. Int J Biol Sci. 2021;17(2):514–26.
42. Datta NS, Williams JL, Caldwell J, Curry AM, Ashcraft EK, Long MW. Novel alterations in cdk1/cyclin b1 kinase complex formation occur during the acquisition of a polyploid DNA content. Mol Biol Cell. 1996;7(2):209–23.
43. Muñoz-Alonso MJ, Ceballos L, Bretones G, Frade P, León J, Gandarillas A. Myc accelerates p21cip-induced megakaryocytic differentiation involving early mitosis arrest in leukemia cells. J Cell Physiol. 2012;227(5):2069–78.
44. Harkin LF, Gerrelli D, Gold Diaz DC, Santos C, Alzu'bi A, Austin CA, et al. Distinct expression patterns for type ii topoisomerases iia and iib in the early foetal human telencephalon. J Anat. 2016;228(3):452–63.
45. Nagai Y, Garrett KP, Ohta S, Bahrun U, Kouro T, Akira S, et al. Toll-like receptors on hematopoietic progenitor cells stimulate innate immune system replenishment. Immunity. 2006;24(6):801–12.
46. Fromowitz A, Aluri S, Gonzalez Lugo JD, Rabinovich E, Ramachandra N, Aminov S, et al. Inhibition of toll-like receptor 4 (tlr4) promotes erythroid and myeloid differentiation in myelodysplastic syndrome (mds) and acute myeloid leukemia (aml). Blood. 2023;142(Suppl 1):5615.
47. Lee JH, Liu R, Li J, Wang Y, Tan L, Li XJ, et al. Egfr-phosphorylated platelet isoform of phosphofructokinase 1 promotes pi3k activation. Mol Cell. 2018;70(2):197-210.e7.
48. Pitchford SC, Lodie T, Rankin SM. Vegfr1 stimulates a cxcr4-dependent translocation of megakaryocytes to the vascular niche, enhancing platelet production in mice. Blood. 2012;120(14):2787–95.
49. Casella I, Feccia T, Chelucci C, Samoggia P, Castelli G, Guerriero R, et al. Autocrine-paracrine vegf loops potentiate the maturation of megakaryocytic precursors through flt1 receptor. Blood. 2003;101(4):1316–23.
50. Sivaraman B, Latour RA. The adherence of platelets to adsorbed albumin by receptor-mediated recognition of binding sites exposed by adsorption-induced unfolding. Biomaterials. 2010;31(6):1036–44.
51. Sivaraman B, Latour RA. Time-dependent conformational changes in adsorbed albumin and its effect on platelet adhesion. Langmuir. 2012;28(5):2745–52.
52. Zenz R, Wagner EF. Jun signalling in the epidermis: from developmental defects to psoriasis and skin tumors. Int J Biochem Cell Biol. 2006;38(7):1043–9.
53. Luff SA, Papoutsakis ET. Megakaryocytic maturation in response to shear flow is mediated by the activator protein 1 (ap-1) transcription factor via mitogen-activated protein kinase (mapk) mechanotransduction. J Biol Chem. 2016;291(15):7831–43.
54. Shen J, Lyu C, Zhu Y, Feng Z, Zhang S, Hoyle DL, et al. Defining early hematopoietic-fated primitive streak specification of human pluripotent

stem cells by the orchestrated balance of wnt, activin, and bmp signaling. J Cell Physiol. 2019;234(9):16136–47.
55. Zhao T, Zhang ZN, Rong Z, Xu Y. Immunogenicity of induced pluripotent stem cells. Nature. 2011;474(7350):212–5.
56. Ito Y, Nakamura S, Sugimoto N, Shigemori T, Kato Y, Ohno M, et al. Turbulence activates platelet biogenesis to enable clinical scale ex vivo production. Cell. 2018;174(3):636-48.e18.
57. Tozawa K, Ono-Uruga Y, Yazawa M, Mori T, Murata M, Okamoto S, et al. Megakaryocytes and platelets from a novel human adipose tissue-derived mesenchymal stem cell line. Blood. 2019;133(7):633–43.
58. Feng Q, Shabrani N, Thon JN, Huo H, Thiel A, Machlus KR, et al. Scalable generation of universal platelets from human induced pluripotent stem cells. Stem Cell Reports. 2014;3(5):817–31.

Publisher's Note